Generalized TLM Algorithms with Controlled Stability Margin and Their Equivalence with Finite-Difference Formulations for Modified Grids

Malgorzata Celuch-Marcysiak and Wojciech K. Gwarek, *Senior Member, IEEE*

***Abstract*— Generalized TLM formulations based on modified grids of 2-D shunt nodes or 3-D expanded nodes are proposed. Generalization consists of permitting flexible control of the numerical stability margin (and thus a time-step for a particular discretization), and of introducing enhanced models for curved boundaries. Formal equivalence between generalized TLM and FDTD algorithms based on the same grids is proved. Simple rules for transforming circuit models (from TLM to FDTD and vice versa) and for their equivalent excitation are given. It is demonstrated that the application of the generalized algorithm reduces computer resources required for the TLM analysis of a circular waveguide by an order of magnitude.**

I. Introduction

THE TLM method is widely used for the modeling of microwave structures. In the classical TLM approach to homogeneous problems, the propagation velocity along each transmission line ($_lv$) is chosen to exceed the physical wave velocity in the modeled medium (v) by a factor of r, with $r = \sqrt{2}$ in a 2-D mesh of shunt nodes and $r = 2$ in a 3-D mesh of expanded nodes. Thus, for a particular discretization of space a, the simulation time-step is stiffly set to $\Delta t = a/_lv = a/(rv)$. In this regard, as noted by several authors [1], [2], more flexibility exists in the FDTD method where the time-step can be controlled by the user.

The first versions of TLM were based on a regular Cartesian grid with a crude staircase approximation of boundaries. Subsequently, other grids have also been utilized, and these can be divided into two categories:

1) rectilinear orthogonal grids with cell dimensions variable as $\Delta x = \Delta x(x)$, $\Delta y = \Delta y(y)$, $\Delta z = \Delta z(z)$; to this category we assign the early technique by Johns [3], the various variable mesh techniques [1], [4] and the recursive algorithm [5];
2) regular grids but in non-Cartesian coordinate systems; this category includes curvilinear orthogonal (e.g., radial) grids [4], [7] and triangular grids [8].

In comparison with the regular Cartesian gridding, the grids of Categories 1 and 2 improve the TLM modeling of many microwave circuits, but they also maintain some limitations. In particular, the grids of Category 1 do not provide the tangential and normal field components for the rigorous specification of boundary conditions at oblique boundaries. The grids of Category 2 are perfectly suited for a narrow class of circuits with all boundaries described by a constant function in one coordinate system. Thus in practical microwave problems of complicated geometry, it often becomes necessary to refine the overall discretization which leads to excessive requirements of computer resources.

Our work addresses these limitations of classical TLM, and proposes original techniques for:

1) controlling factor r introduced above—which has a mathematical interpretation of controlling a stability margin and a physical interpretation of controlling the simulation time-step.
2) improving the representation of arbitrary curved boundaries through the introduction of locally modified grids.

In the MTT-S paper [9], we approached the problem of the controlled stability margin by developing the complete dispersion relations for the stub-loaded TLM, which required cumbersome arithmetic. The new boundary model was established by incorporating local integral approximations into TLM [9]. A unified approach to both problems presented herein is substantially more general and effective.

We shall first postulate the existence of the generalized TLM algorithms based on modified grids. We shall conduct a formal proof of their equivalence with FDTD algorithms (based on the same grids), and derive simple rules for transformation between the FDTD and TLM models. These rules enable immediate formulation of the TLM algorithms with controlled stability margin and with flexible representation of curved boundaries, originally proposed for FDTD [10], [11]. In derivations we shall concentrate on 2-D problems. Conclusions will be directly extended to the 3-D expanded node (ExpN) which is a combination of the 2-D shunt and series nodes.

In the final example of a circular waveguide, we relate our generalized TLM formulations based on modified grids to classical FDTD and TLM, and to nonorthogonal FDTD of [12]. To our knowledge, this is the first in the literature comparison of accuracy of the locally and globally irregular grids for the time-domain modeling.

II. Generalized TLM Algorithms

Consider an arbitrarily shaped 2-D circuit of Fig. 1(a). Its boundaries can be short, open, or resistive (which provides

Manuscript received October 8, 1994; revised May 25, 1995. This work is supported in part by the Commission of the European Communities Contract Copernicus: 7565.

The authors are with the Institute of Radioelectronics, Warsaw University of Technology, Nowowiejska 15/19, 00-665 Warsaw, Poland.

IEEE Log No. 9413410.

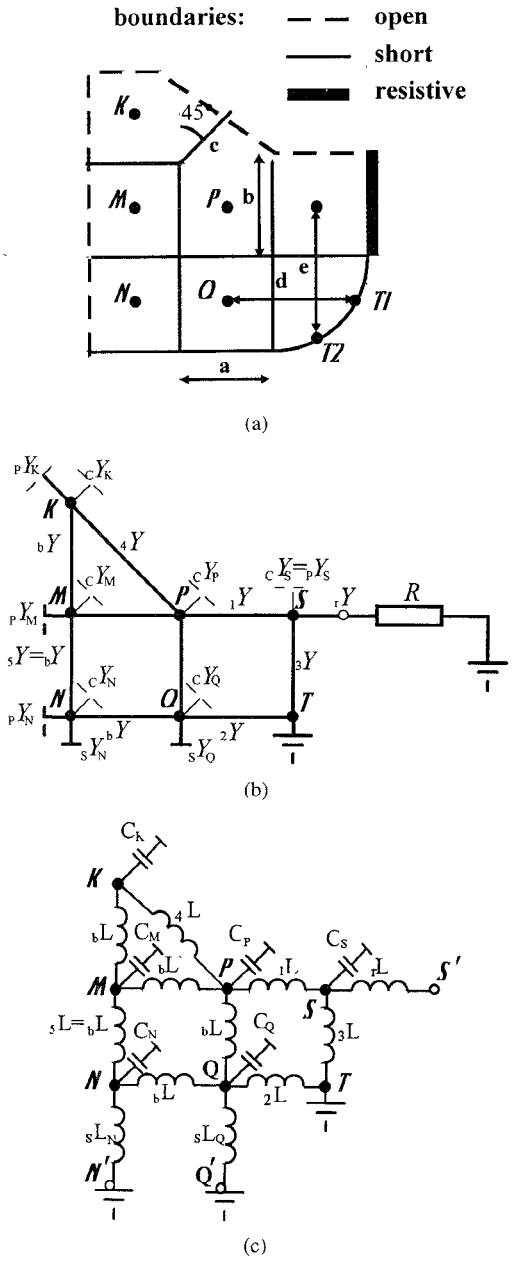

Fig. 1. (a) An arbitrarily shaped 2-D microwave circuit; (b), its TLM model proposed herein, (c) and an equivalent FDTD model.

in particular a narrow band model of a matched termination or a lossy metal surface [6]). Upon this circuit we impose a fundamentally orthogonal grid with possible use of variable mesh techniques, and we match the curved boundary by means of modified nonrectangular cells [Fig. 1(a)].

Generalizing the classical TLM approach and our recent contribution [9], we claim that the circuit of Fig. 1(a) can be modeled by a matrix of transmission lines shown in Fig. 1(b). In the matrix we distinguish two types of lines (branches): link lines and stubs. Consider node $\mathcal{N}$ with total number N_b of incident branches of any types and any characteristic admittances ${}_bY_N$. A pulse ${}^r_bV^k_N$ scattered into branch b at time instant $k\Delta t$ is calculated as

$$ {}^r_bV^k_N = u^k_N - {}^i_bV^k_N \qquad b = 1, \cdots, N_b \tag{1} $$

where ${}^i_bV^k_N$ is the incident pulse and u^k_N denotes nodal voltage defined as

$$ u^k_N = \frac{2}{\sum_{b=1}^{N_b} {}_bY_N} \sum_{b=1}^{N_b} {}_bY_N {}^i_bV^k_N. \tag{2} $$

In (1), (2) and further in the paper, subscripts refer to nodes, prescripts, to branches, and superscripts, to time instants.

If the TLM simulation is conducted with time-step Δt, then each link branch introduces a propagation delay of Δt and each stub $-\Delta t/2$. Thus, the connection equations take the form

$$ {}^i_lV^{k+1}_N = {}^r_lV^k_M \tag{3} $$

$$ {}^i_lV^{k+1}_M = {}^r_lV^k_N \tag{4} $$

for link branch l connecting nodes $\mathcal{N}$ and $\mathcal{M}$, and

$$ {}^i_pV^{k+1}_N = {}^r_pV^k_N \tag{5} $$

$$ {}^i_sV^{k+1}_N = -{}^r_sV^k_N \tag{6} $$

$$ {}^i_mV^{k+1}_N = 0 \tag{7} $$

$$ {}^i_rV^{k+1}_N = \frac{R_rY_N - 1}{R_rY_N + 1} {}^r_rV^k_N \tag{8} $$

for open (p), short (s), matched (m) and resistively terminated (r) stubs at node $\mathcal{N}$, respectively.

In the classical TLM modeling, link branches are parallel to the coordinate axes. Their different characteristic admittances result from inhomogeneous permeability or variable dimensions of cells [1]. Stubs have the following meaning:

- open stubs p model inhomogeneous permittivity or magnetic boundary,
- short stubs s model electric boundaries (in 3-D, short stubs at series nodes also model inhomogeneous permeability),
- matched stubs m model dielectric losses,
- resistively terminated stubs r model resistive boundaries or an actual lumped element incorporated into the circuit.

Our generalization consists in allowing that:

1) link branches can be placed obliquely in the matrix, in order to model the flow of the current tangential to the open boundary [${}_4Y$ in Fig. 1(b)],
2) double-node cells can be used to represent the curved electric boundary ($\mathcal{T}$ in Fig. 1),
3) additional open stubs (in 3-D, also short stubs) can be used to control a stability margin and thus a time-step of the algorithm.

These extensions to classical TLM will be explained in the following sections, via the equivalence with the FDTD formulations.

III. Equivalence of TLM and FDTD Formulations for Modified Grids

Equations (1)–(8) applied to a model of Fig. 1(b) with chosen initial conditions describe the TLM simulation of fields in the circuit of Fig. 1(a). We will prove that a formally equivalent simulation can be conducted in the FDTD method. By formal equivalence, we mean that with the use of infinitely precise computer arithmetic, both methods would provide identical field values at any time instant and at any location.

In this work, we shall not compare the numerical robustness of FDTD and TLM with respect to the computer round-off errors. This topic has been briefly addressed in [13], and it is worth further systematic research. However, our experience shows that in typical microwave problems the two methods are immune to computer round-off errors, even if single precision arithmetic is used [14]. Therefore, their formal equivalence is a concept of practical as well as cognitive importance.

Criteria for formal equivalence of the TLM and FDTD methods concern two aspects: equivalent transformation of the model and equivalent transformation of the initial conditions. We shall discuss the two aspects separately. In the discussion we shall refer to the FDTD notation introduced in [10]. This notation uses auxiliary variables: voltage and currents. Voltage is defined as

$$u = \int E_z \, dz = E_z h \tag{9}$$

where h is the height of a planar circuit. Surface current density is related to the transverse H-field by

$$\overline{j}_\perp = \overline{i}_z \times \overline{H}_\perp. \tag{10}$$

Current flowing between two nodes is the integral of $\overline{j}_\perp$ along the common side of respective two cells, for example [c.f., Fig. 1(c)]

$$_1i = {}_1j_x b. \tag{11}$$

The FDTD model is a network of nodal capacitances and branch inductances [10]. The effects of inhomogeneous filling and variable dimensions of cells are described by modified values of C_N and ${}_bL$. The value of a in the FDTD equations denotes a fundamental cell size in the model (which is not necessarily the smallest size).

A. Equivalent Transformation of the Model

Equivalent transformation of the TLM model of Fig. 1(b) into the FDTD model of Fig. 1(c) is governed by the following criteria

1) At each node $\mathcal{N}$ with incident N_l link branches l, N_p open branches p, N_s short branches s, N_r resistively loaded branches r and N_m matched branches m we place capacitance C_N such that

$$\frac{\Delta t}{C_N a} = \frac{2}{\sum_{l=1}^{N_l} {}_lY_N + \sum_{p=1}^{N_p} {}_pY_N + \sum_{s=1}^{N_s} {}_sY_N + \sum_{r=1}^{N_r} {}_rY_N} \tag{12}$$

and conductance G_N such that

$$G_N = \sum_{m=1}^{N_m} {}_mY_N. \tag{13}$$

2) Each link branch of characteristic admittance ${}_lY$ is replaced by inductance ${}_lL$ such that

$$\frac{\Delta t}{{}_lLa} = {}_lY. \tag{14}$$

3) Open branches are neglected (their influence is included in (12)).

4) Each branch ${}_rY$ ended with resistance R or short-ended ($R = 0$) is replaced by inductance ${}_rL$

$$\frac{\Delta t}{{}_rLa} = \frac{2{}_rY}{1 + {}_rYR} \tag{15}$$

while at the resistive end we place an auxiliary node $\mathcal{N}'$ where at the nodal voltage $u_{N'}$ is explicitly defined by

$$u_{N'}^k = -R_r i_N^{k-0.5} \tag{16}$$

and ${}_ri_N$ denotes current flowing out of R, towards $\mathcal{N}$.

Formal proof of the equivalence of this transformation is given in the Appendix.

Let us now extend the discussion to the 3-D ExpN modeling. At shunt nodes criteria (12), (13), (15), and (16) (and the associated steps 1, 3 of the proof) remain valid. At series nodes, dual reasoning can be applied. Normally, incident at series node $\mathcal{M}$ are M_l link branches and M_s short stubs. In the FDTD model, at node $\mathcal{M}$ we locate nodal inductance L_M defined as

$$\frac{\Delta t}{L_M a} = \frac{2}{\sum_{l=1}^{M_l} {}_lZ_M + \sum_{s=1}^{M_s} {}_sZ_M} \tag{17}$$

and we neglect short branches.

B. Equivalent Modeling of Initial Conditions

In the FDTD method, initial conditions must be given for nodal voltages at $k = 0$ and branch currents at $k = -0.5$. In TLM, initial conditions are completely defined by the values of all incident pulses in the model at a single time instant $k = 0$. Physically, this corresponds to enforcing the values of both voltage and current in the middle of each branch at $k = -0.5$. Thus at first sight it seems that FDTD and TLM cannot be excited in the same way, and this point has been raised in previous comparisons of the two methods [15]. We will now resolve such doubts by showing that any excitation in TLM has an equivalent in FDTD. By "equivalent excitation" we understand such a definition of initial voltages and currents in FDTD, and of initial incident pulses in TLM which result in identical field values obtained with the two methods at any location and at any time instant $k > 0$. We shall refer to the initial TLM excitation from one branch by a single delta pulse, remembering that any other excitation waveform consists of a train of pulses, and our conclusions will apply by virtue of superposition.

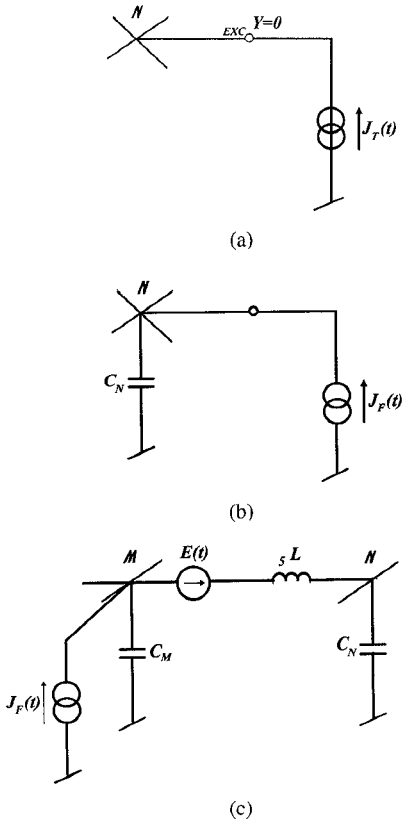

Fig. 2. Excitation schemes for TLM and FDTD applied to the circuit of Fig. 1, (a) TLM excitation of node $\mathcal{N}$ from current source: $J_T(t) = 2\delta(t + 0.5\Delta t)$, (b) FDTD excitation equivalent to (a): $J_F(t) = 2[\delta(t + 0.5\Delta t) + \delta(t - 0.5\Delta t)]$, (c) FDTD excitation of node $\mathcal{N}$ from branch $_5L$, equivalent to TLM excitation by $\frac{1}{5}V_N^0 = 1$: $E(t) = \delta(t + \Delta t)$, $J_F(t) = \delta(t + 0.5\Delta t)$.

TABLE I
NODAL VOLTAGES AND BRANCH CURRENTS OBTAINED FOR THE CIRCUIT OF FIG. 1 BY BOTH TLM AND FDTD, AS A RESULT OF EXCITATIONS OF FIG. 2(a) AND FIG. 2(b), RESPECTIVELY. CONSIDERED ARE MODELS OF FIG. 1(b) AND FIG. 1(c) WITH $_bY = 1$, $\frac{\Delta t}{a_bL} = 1$, $_CY_N = {}_CY_M = {}_CY_Q = 0$, $\frac{\Delta t}{aC_N} = \frac{\Delta t}{aC_N} = \frac{\Delta t}{aC_N} = \frac{1}{2}$

k	u_N	u_M	u_Q	s^1_N	s^1_N
-0 5				0 00	0 00
0	1.00	0.00	0.00		
0 5				-1 00	-2.00
1	0 00	0 50	0 50		
1 5				-0 50	-2.00
2	-1 50	0 25	-0 25		

First, we consider the excitation of node $\mathcal{N}$ of Fig. 1 from the ideal current source connected by an additional stub $_{exc}Y = 0$ [Fig. 2(a)]. All other incident pulses at $k = 0$ are set to zero. Clearly, the excitation stub does not influence further analysis. The values of selected voltages and currents in the circuit of Fig. 1, as produced by TLM at the beginning of the simulation, are given in Table I.

The same sequence of nodal voltages and branch currents (Table I) is produced by FDTD if the excitation scheme of Fig. 2(b) is incorporated. This means that for the equivalence with TLM, in the FDTD modeling the same delta pulse excitation must be applied to node $\mathcal{N}$ at $k = 0$ and repeated at $k = 1$.

Let us consider what happens if both TLM and FDTD are excited by a single pulse at $k = 0$. We denote by $U_{\mathrm{TLM}}(t)$ and $U_{\mathrm{FDTD}}(t)$ signals detected at a particular location in the circuit (for example voltage at node $\mathcal{N}$). In view of the above discussion, $U_{\mathrm{TLM}}(t) = U_{\mathrm{FDTD}}(t) + U_{\mathrm{FDTD}}(t - \Delta t)$ and the following relation between their effective spectra holds

$$\begin{aligned} |\mathcal{F}[U_{\mathrm{TLM}}(t)]| &= |\mathcal{F}[U_{\mathrm{FDTD}}(t) + U_{\mathrm{FDTD}}(t - \Delta t)]| \\ &= |\mathcal{F}[U_{\mathrm{FDTD}}(t)]| \circ |1 + \exp(-j2\Pi f \Delta t)| \\ &= |\mathcal{F}[U_{\mathrm{FDTD}}(t)]| \circ |\cos(\Pi f \Delta t)|. \end{aligned} \tag{18}$$

From this follows an interesting conclusion that a single pulse excitation in TLM produces signals of cosinusoidally modulated spectra, with respect to signal s produced in FDTD by the same single pulse source. In some circuits strong resonances can be grouped above the frequency band of interest, at frequencies approaching the Nyquist point $f_N = 1/(2\Delta t)$. With all excited signals having modulated spectra of the form (18), the effect of numerical "ringing" at these resonances is diminished, and consequently the convergence of calculations improves [14]. This may explain better convergence of TLM reported in examples using a single pulse excitation in both TLM and FDTD [15], [16]. Naturally, equivalent excitation models as specified above provide identical convergence of FDTD and TLM.

An alternative TLM excitation is by a pulse incident from one of the link lines, for example from line $_5Y_N$ at one node $\mathcal{N}$ of Fig. 1. An FDTD equivalent again comprises a two-pulse excitation, applied to branch current at $k = -0.5$ and to nodal voltage at $k = 0$ [Fig. 2(c)].

C. Consequences of Formal Equivalence

In view of formal equivalence, the TLM and FDTD methods exhibit identical properties in terms of stability, energy conservation, and flexibility in the modeling of irregular geometries. Therefore by direct transformation from FDTD, techniques for controlling the stability margin and improving the curved boundary representation will be incorporated into TLM.

D. A Spurious TLM Mode and Its Effect on Formal Equivalence with FDTD

As a consequence of using more variables, the TLM method has more eigenvalues than FDTD, and it emulates spurious modes which do not exist in FDTD. In a previous paper [17] we have shown that the TLM spurious modes are described by the dispersion term $\sin(2\Pi f \Delta t) = 0$, thus they are supported at $f = 1/(2\Delta t)$. However, the TLM spurious modes do not violate formal equivalence with FDTD. They are characterized by zero nodal voltages and zero branch currents which are our variables of interest. Furthermore, they are nonpropagating modes and cause the oscillations of branch voltages only where specifically excited. We have established these properties by examining the complete TLM characteristic equation given in [9].

IV. Controlled Stability Margin in TLM

Consider a homogeneous region of space covered by a Cartesian grid of cell size a. We construct its 2-D TLM model with link branches ${}_bY$ and open stubs ${}_CY$. In a 3-D TLM model we additionally admit short stubs ${}_LZ$ at series nodes. All parameters ${}_bY$, ${}_CY$, ${}_LZ$ as well as L, C in FDTD are constant throughout the model.

For the FDTD solutions, the numerical dispersion relations have been investigated by several authors [2], [14], [18]. A fundamental parameter of these relations is a stability factor r defined as

$$r^2 = \frac{aC}{\Delta t}\frac{aL}{\Delta t} = \left[\frac{\frac{a}{\Delta t}}{v}\right]^2. \tag{19}$$

The FDTD calculations are stable [2], [14], [18], and [19] and numerical energy is conserved [19], [20] in 2-D if $r \geq \sqrt{2}$, and in 3-D if $r \geq \sqrt{3}$. By a stability margin of the algorithm we shall understand the interval $\langle\sqrt{2},\ r\rangle$ in 2-D and $\langle\sqrt{3},\ r\rangle$ in 3-D.

Note that (19) is consistent with the definition of factor r proposed for TLM in the introduction since

$$r = \frac{\frac{a}{\Delta t}}{v} = \frac{lv}{v}. \tag{20}$$

Applying equivalence criteria (12), (14) we can express a stability factor in terms of characteristic admittances of the TLM branches in 2-D

$$r^2 = \frac{4{}_bY + {}_CY}{2}\frac{1}{{}_bY} = \frac{1}{2}\left[4 + \frac{{}_CY}{{}_bY}\right]. \tag{21a}$$

In 3-D, we apply criteria (12), (17)

$$r^2 = \frac{4{}_bY + {}_CY}{2}\frac{4 + {}_bY\,{}_LZ}{2{}_bY} = \frac{1}{4}\left[4 + \frac{{}_CY}{{}_bY}\right][4 + {}_bY\,{}_LZ]. \tag{21b}$$

Expressions for r identical to (21) have been originally obtained in our MTT-S paper [9] by cumbersome trigonometric transformations of the TLM dispersion relations for the 3-D model with stubs. In previous papers, only the 2-D stub-loaded TLM model has been considered [2], and conclusions concerning the possibility to control the time-step have not been drawn.

Based on (21), we draw the following conclusions:

1) We confirm that classical TLM without stubs (${}_CY = 0$, ${}_LZ = 0$) is operated in 2-D at $r = \sqrt{2}$ and in 3-D at $r = 2$.
2) In 2-D and 3-D TLM, it is possible to increase a stability margin through the use of positive stubs. Thereby we obtain a family r^+ of TLM algorithms, discussed in the following section.
3) Using negative stubs, we can formulate a family r^- of stable 3-D TLM algorithms with decreased stability margin ($\sqrt{3} \leq r < 2$).

Let us first consider the TLM algorithms of *family* r^-. Compared with classical 3-D ExpN TLM, they exhibit two advantages:

TABLE II
Errors in Calculating Eigenfrequencies of a 14×14×20 mm Cavity with 3-D TLM (a =2 mm)

mode	f_{ph} [GHz]	$r = \sqrt{3}$ δf [%]	$r = 2$ δf [%]
101	13.078	-0 21	-0 31
110	15 152	-0 24	-0.38
111	16 907	-0 04	-0 21

- numerical dispersion errors decrease as in the FDTD method [2], [14], and [18],
- simulation can be conducted with the time-step prolonged by a factor of $2/\sqrt{3}$, thus the total number of iterations is reduced by up to 13%.

A limitation of the r^- algorithms is that they permit the modeling of electric walls only through the planes where tangential electric fields are defined, and of magnetic walls through the planes where tangential magnetic fields are defined. This limitation follows from the range of elements admitted in constructing the TLM model. Thus the r^- algorithms are suitable for circuits of fairly regular geometry.

In Table II we show eigenfrequencies of a 14×14×20 mm cavity calculated by standard TLM ($r = 2$) and r^- TLM ($r = \sqrt{3}$). For both algorithms we have used the same cell size $a = 2$ mm and the same scheme for initial excitation and parameter extraction, as introduced in [21]. This scheme is based on incorporating an auxiliary lossy voltage source and detecting the eigenfrequencies as minima of the discrete Fourier transform of the input current [21]. Note that the version with $r = \sqrt{3}$ remains stable despite the use of negative stubs (${}_bY = 1$, ${}_LZ = 0$, ${}_CY = -1$), and it provides more accurate results (Table II).

V. Improved TLM Modeling of Curved Boundaries

Algorithms of *family* r^+ enforce an extra stability margin into the TLM method. This margin can serve to accommodate improved models of arbitrarily shaped boundaries. In the 2-D FDTD method, a very flexible model as in Fig. 1(c) has been developed for open [10] and short [11] boundaries. Parameters L, C of this model are obtained by assuming local quasistatic field distribution over each cell. Consequently, L, C have the physical meaning of quasistatic inductances between nodes, and quasistatic capacitances of cells [10]. Applying the equivalence criteria, we can immediately transform this FDTD model into the TLM model of Fig. 1(b).

Let us assume that in regions covered by a regular square grid, standard values of ${}_bL$ and C_M in FDTD are chosen so that

$$\frac{\Delta t}{a\,{}_bL} = 1 \tag{22}$$

$$\frac{\Delta t}{aC_M} = \frac{1}{r^2} \tag{23}$$

where r is the desired stability factor; relations (22), (23) satisfy (19).

Applying the branch equivalence criterion (14), we obtain characteristic admittance of standard link lines as

$$_bY = 1. \tag{24}$$

Between distorted cells, quasi-static inductance is modified which results in modified branch admittance, for example

$$\frac{\Delta t}{a_1 L} = {}_1Y = \frac{b}{a} \tag{25}$$

$$\frac{\Delta t}{a_2 L} = {}_2Y = \frac{a}{d}. \tag{26}$$

A unique feature of our model is that it contains oblique branches which allow for the flow of a current tangential to the open boundary, such as $_4L$, $_4Y$

$$\frac{\Delta t}{a_4 L} = {}_4Y = \frac{c}{a\sqrt{2}}. \tag{27}$$

In this way, all link branches and stubs perpendicular to the boundaries in Fig. 1(b) are defined. Finally, the nodal equivalence criterion (12) is applied to define permittivity/stability stubs. For regular cell $\mathcal{M}$ we have

$$\frac{\Delta t}{aC_M} = \frac{2}{2_bY + {}_pY_M + {}_sY_M + {}_CY_M} = \frac{2}{4_bY + {}_CY_M}. \tag{28}$$

Taking into account (23), (24)

$$_CY_M = 2r^2 - 4. \tag{29}$$

At other nodes we obtain for example

$$_CY_P = 2r^2 S_P - [2 + {}_4Y + {}_1Y] \tag{30}$$

where S_P denotes cell area normalized to standard cell area a^2.

The value of $r = 2$ is always sufficient to avoid negative stubs and to maintain stability.

A. Remarks on Inhomogeneous Problems

For clarity we have so far concentrated on homogeneous circuits, but our study also applies to inhomogeneous problems. As explained in [10], the FDTD values of nodal capacitances and branch inductances increase proportionally to ε_r and μ_r, respectively. Then the equivalence criteria (12)–(17) define modified values of branch admittances in TLM. For example, if relative permeability of the region between nodes $\mathcal{P}$ and $\mathcal{S}$ in Fig. 1(a) is increased by a factor of μ_1, then $_1Y$ is given by (31) instead of (25)

$$\frac{\Delta t}{a_1 L} = {}_1Y = \frac{1}{\mu_1}\frac{b}{a}. \tag{31}$$

Similarly, if relative permittivity of the medium filling cell $\mathcal{P}$ is increased by a factor of ϵ_P, then stub $_CY_P$ is defined by (32) instead of (30)

$$_CY_P = 2r^2 S_P \epsilon_P - [2 + {}_4Y + {}_1Y]. \tag{32}$$

TABLE III
ERRORS IN CALCULATING CUTOFF FREQUENCIES OF TE-MODES IN A CIRCULAR WAVEGUIDE OF $R = 1$ M BY THE 2-D TLM METHOD

physical values		STAIR-CASE BOUNDARY, $r = \sqrt{2}$			NEW BOUNDARY MODEL, $r = 2$		
		δf [%]			δf [%]		
mode	f_{ph} [GHz]	$R/a = 5$	$R/a = 10$	$R/a = 20$	$R/a = 5$	$R/a = 10$	$R/a = 20$
H_{11}	0.0879	- 2.39	- 1.02	0 00	0 11	0 00	0 00
H_{21}	0.1458	-13 45	- 4 33	- 1.73	- 1 04	- 0.29	- 0 08
H_{01}	0.1829	*	1 11	0.57	- 0.74	- 0.20	- 0.09
H_{31}	0.2005	12 27	- 2 88	- 0 59	- 1 24	- 0 39	- 0.14

Thus, the stub accounts in a multiplicative way for two physical factors:

1) increased permittivity of the modeled medium,
2) decreased simulation time-step Δt (increased r for the fixed medium and spatial discretization a).

B. Practical Advantages of the New Boundary Model

We calculate cutoff frequencies of modes in a circular waveguide of radius R, using successively refined discretization a. For the TM modes, this is a 2-D problem with short boundary conditions; for the TE modes—a dual 2-D problem with open boundary conditions. We define an error of the analysis as

$$\delta f = \frac{f - f_{\rm ph}}{f_{\rm ph}} \tag{33}$$

where f, $f_{\rm ph}$ are the calculated and physical values of frequency. As in Section IV, the excitation scheme after [21] combined with the discrete Fourier transform is used.

First, we consider the TE modes by:

1) standard 2-D TLM with $r = \sqrt{2}$ and a staircase boundary model,
2) TLM with $r = 2$ and the new boundary model.

Results are shown in Table III. For comparable accuracy, standard TLM requires refinement of the discretization by a factor of 2–4, and this leads to the increase of computer memory and time requirements by factors of 4–16 and 8–64, respectively. On the other hand, our curved boundary model requires only slight modification of the standard TLM code, and imposes practically no additional requirements on computer resources. The effect of increased numerical dispersion due to increased r becomes negligible, in comparison with the improved boundary representation.

Further, for the TM_{01} mode ($f_{\rm ph} = 0.1149$ GHz for $R = 1$ m) we conduct a systematic convergence study comparing the following approaches:

1) classical TLM or FDTD based on a regular Cartesian grid with staircase approximation of the boundary defined only at nodes,
2) classical TLM based on a regular Cartesian grid with staircase approxim ation of the boundary, with boundary defined at nodes or bisecting branches,
3) our TLM (FDTD) formulation based on a locally modified grid,
4) nonorthogonal FDTD [12] based on a globally irregular grid.

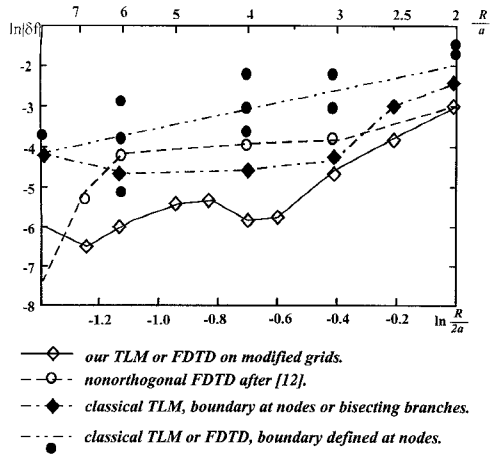

Fig. 3. Errors in calculating cutoff frequency of the TM_{01} circular waveguide mode, as a function of discretization.

Errors due to approaches (1)–(4) are plotted in Fig. 3. Application of the locally modified grids discussed in this paper leads to the most accurate FDTD and TLM numerical schemes. In comparison with nonorthogonal FDTD, these schemes require approximately half of computer memory and one third of computing time (for the same number of cells in the model).

In case 1 which involves crude boundary approximation, results strongly depend on the positioning of the model with respect to basic grid lines, and we have marked various results by dots in Fig. 3. A straight line repeated for classical FDTD after [12] represents average errors. Results become unambiguous for refined discretization and improved boundary models.

VI. Conclusion

We have proved formal equivalence between the generalized TLM (for shunt or expanded node) and FDTD formulations based on modified grids. Simple rules for transforming circuit models (from TLM to FDTD and vice versa) and for their equivalent excitation have been given. It must be emphasized that these rules clarify many previous misunderstandings concerning relationships between the FDTD and TLM methods, and their applicability extends far beyond specific topics of this paper.

Formal equivalence with FDTD reveals the possibility to control a stability margin in the TLM algorithms. Algorithms of *family* r^- with the decreased stability margin reduce the numerical dispersion errors and computing time for regularly shaped 3-D microwave circuits. Algorithms of *family* r^+ enable stable incorporation of enhanced models for curved boundaries. One such a model has been transformed from the generalized FDTD method into TLM.

According to the authors' experience, the TLM algorithms with the new boundary model (as well as the equivalent FDTD algorithms based on the approach of [10], [11]) are competitive tools for the analysis of irregularly shaped microwave

$$u_N^{k+1} = \frac{2}{\sum_{l=1}^{N_l} {}_l Y_N + \sum_{p=1}^{N_p} {}_p Y_N + \sum_{s=1}^{N_s} {}_s Y_N + \sum_{r=1}^{N_r} {}_r Y_N + \sum_{m=1}^{N_m} {}_m Y_N} \cdot \left[\sum_{l=1}^{N_l} {}_l Y_{N\,l}^{\,i} V_N^{k+1} + \sum_{p=1}^{N_p} {}_p Y_{N\,p}^{\,i} V_N^{k+1} + \sum_{s=1}^{N_s} {}_s Y_{N\,s}^{\,i} V_N^{k+1} + \sum_{r=1}^{N_r} {}_r Y_{N\,r}^{\,i} V_N^{k+1} \right] \tag{A1}$$

$$u_N^{k} = \frac{2}{\sum_{l=1}^{N_l} {}_l Y_N + \sum_{p=1}^{N_p} {}_p Y_N + \sum_{s=1}^{N_s} {}_s Y_N + \sum_{r=1}^{N_r} {}_r Y_N + \sum_{m=1}^{N_m} {}_m Y_N} \cdot \left[\sum_{l=1}^{N_l} {}_l Y_{N\,l}^{\,r} V_N^{k} + \sum_{p=1}^{N_p} {}_p Y_{N\,p}^{\,r} V_N^{k} + \sum_{s=1}^{N_s} {}_s Y_{N\,s}^{\,r} V_N^{k} + \sum_{r=1}^{N_r} {}_r Y_{N\,r}^{\,r} V_N^{k} + \sum_{m=1}^{N_m} {}_m Y_{N\,m}^{\,r} V_N^{k} \right]. \tag{A2}$$

$$u_N^{k+1} = \frac{\sum_{l=1}^{N_l} {}_l Y_N + \sum_{p=1}^{N_p} {}_p Y_N + \sum_{s=1}^{N_s} {}_s Y_N + \sum_{r=1}^{N_r} {}_r Y_N - \sum_{m=1}^{N_m} {}_m Y_N}{\sum_{l=1}^{N_l} {}_l Y_N + \sum_{p=1}^{N_p} {}_p Y_N + \sum_{s=1}^{N_s} {}_s Y_N + \sum_{r=1}^{N_r} {}_r Y_N + \sum_{m=1}^{N_m} {}_m Y_n} u_N^{k} + \frac{2}{\sum_{l=1}^{N_l} {}_l Y_N + \sum_{p=1}^{N_p} {}_p Y_N + \sum_{s=1}^{N_s} {}_s Y_N + \sum_{r=1}^{N_r} {}_r Y_N + \sum_{m=1}^{N_m} {}_m Y_N} \cdot \left[\sum_{l=1}^{N_l} {}_l i_N^{k+0\,5} + \sum_{s=1}^{N_s} {}_s i_N^{k+0.5} + \sum_{r=1}^{N_r} {}_r i_N^{k+0\,5} \right]. \tag{A3}$$

structures. For a circular waveguide considered in this paper, accurate results have been obtained with only about 10% of computer resources required by standard TLM or FDTD with a staircase boundary approximation. In the same example, the generalized algorithms have been shown more accurate than the nonorthogonal FDTD method of [12], despite higher requirements of computer resources of the latter one.

APPENDIX

Consider generalized TLM and FDTD models of Fig. 1(b), (c). We assume that at time $k\Delta t$ all nodal voltages are equal in TLM and FDTD, and at time $(k+0.5)\Delta t$—all branch currents. The values of individual TLM pulses producing these voltages and currents are unimportant. We also assume that calculations are conducted with infinite precision.

Step 1 : We shall prove that nodal voltages calculated at $(k+1)\Delta t$ by the FDTD and TLM algorithms will be equal.

In the TLM algorithm we can express nodal voltage in terms of incident pulses as in (A1) shown at the bottom of the preceding page or in terms of reflected pulses as in (A2) shown at the bottom of the preceding page. We subtract (A2) from (A1) and take into account (5), (7) as in (A3) also shown at the bottom of the preceding page. Currents ${}_li_N$ are defined in the middle of link branches l, currents ${}_si_N$, ${}_ri_N$—at the short or resistively-terminated ends of branches s, r, respectively. On the other hand, an FDTD equation for node $\mathcal{N}$ produces the value $\tilde{u}_N^{k+1}$

$$\tilde{u}_N^{k+1} = \frac{C_N\frac{a}{\Delta t} - \frac{1}{2}G_N}{C_N\frac{a}{\Delta t} + \frac{1}{2}G_N}u_N^k + \frac{1}{C_N\frac{a}{\Delta t} + \frac{1}{2}G_N} \cdot \left[\sum_{l=1}^{N_l} {}_li_N^{k+0\,5} + \sum_{s=1}^{N_s} {}_si_N^{k+0.5} + \sum_{r=1}^{N_r} {}_ri_N^{k+0\,5}\right]. \quad \text{(A4)}$$

In view of our assumption for u_N^k and all ${}_li_N^{k+0.5}$, ${}_si_N^{k+0.5}$, ${}_ri_N^{k+0\,5}$ we find

$$\tilde{u}_N^{k+1} = u_N^{k+1} \quad \text{(A5)}$$

if and only if nodal equivalence criteria (12), (13) are satisfied.

Step 2 : We shall prove that currents ${}_li^{k+1.5}$ in link branches further calculated by FDTD and TLM will be equal.

We consider current ${}_li$ flowing in branch l from node $\mathcal{M}$ to $\mathcal{N}$. In terms of the TLM pulses we can write

$${}_li^{k+0\,5} = -{}_lY[{}_l^rV_N^k - {}_l^rV_M^k] \quad \text{(A6)}$$

$${}_li^{k-0.5} = {}_lY[{}_l^iV_N^k - {}_l^iV_M^k]. \quad \text{(A7)}$$

Thus, updating of TLM branch currents is governed by the relation

$${}_li^{k+0.5} = {}_li^{k-0\,5} + {}_lY[u_M^k - u_N^k]. \quad \text{(A8)}$$

This is equivalent to updating currents in FDTD if and only if branch equivalence criterion (14) is met.

Step 3 : We shall prove that also currents in short- and resistively-ended branches at $(k+1.5)$ will be equal in FDTD and TLM.

Consider branch r incident at node $\mathcal{N}$ and terminating in resistance R. In a special case of $R=0$ it reduces to a short-ended branch s. In TLM algorithm terminal current in this branch can be expressed as

$${}_ri_N^{k+0.5} = {}_rY[{}_r^iV_N^{k+1} - {}_r^rV_N^k] \quad \text{(A9)}$$

$${}_ri_N^{k-0.5} = {}_rY[{}_r^iV_N^k - {}_r^rV_N^{k-1}]. \quad \text{(A10)}$$

Additionally we know that

$${}_r^iV_N^{k+1} = \frac{R_rY-1}{R_rY+1}{}_r^rV_N^k \quad \text{(A11)}$$

$${}_r^rV_N^{k-1} = \frac{R_rY+1}{R_rY-1}{}_r^iV_N^k. \quad \text{(A12)}$$

From (A9)–(A12):

$${}_ri_N^{k+0\,5} + \frac{R_rY-1}{R_rY+1}{}_ri_N^{k-0\,5} = {}_rY\frac{-2}{R_rY+1}u_N^k \quad \text{(A13)}$$

$${}_ri_N^{k+0\,5} = {}_ri_N^{k-0.5} + \frac{2_rY}{R_rY+1}[-R_r{}_ri_N^{k-0.5}] - \frac{2_rY}{R_rY+1}u_N^k. \quad \text{(A14)}$$

According to (16) we define an auxiliary node $\mathcal{N}'$ and obtain

$${}_ri_N^{k+0\,5} = {}_ri_N^{k-0.5} + \frac{2_rY}{R_rY+1}[u_{N'}^k - u_N^k]. \quad \text{(A15)}$$

If criterion (15) is met, equation (A15) is equivalent to an FDTD equation.

Step 4 : Resorting to the principle of mathematical induction, we find that nodal voltages and branch currents at all successive time-instants are equal in FDTD and TLM.

REFERENCES

[1] R. H. Voelker and R. J. Lomax, "A finite-difference transmission line matrix method incorporating a nonlinear device model," *IEEE Trans. Microwave Theory Tech.*, vol. 38, no. 3, pp. 302–312, Mar. 1990.

[2] N. R S Simons and E. Bridges, "Equivalence of propagation characteristics for the transmission-line matrix and finite-difference time-domain methods in two dimensions," *IEEE Trans. Microwave Theory Tech.*, vol. MTT-39, no. 2, pp. 354–357, Feb. 1991.

[3] P. B. Johns and G. F. Slater, "Transient analysis of waveguides with curved boundaries," *Electron. Lett.*, vol. 9, no. 21, pp. 486–487, Oct. 1973.

[4] D. A. Al-Mukhtar and J E. Sitch, "Transmission-line matrix method with irregularly graded space," *Proc. Inst. Elec Eng.*, pt. H, vol. 128, no 6, pp. 299–305, Dec. 1981.

[5] U. Mueller, A. Beyer, and W. J. R. Hoefer, "Moving boundaries in 2-D and 3-D TLM simulations realized by recursive formulas," *IEEE Trans. Microwave Theory Tech.*, vol. 40, no. 12, pp. 2267–2271, Dec. 1992.

[6] W. J. R. Hoefer, "The transmission line matrix method—theory and applications," *IEEE Trans. Microwave Theory Tech.* , vol. MTT-33, no. 10, pp. 882–892, Oct. 1985.

[7] H. Meliani, D. De Cogan, and P. B. Johns, "The use of orthogonal curvilinear meshes in TLM models," *Int. J. Numerical Modelling: Electron, Networks, Devices, and Fields*, vol. 1, pp. 221–238, 1988.

[8] N. R S Simons and A. A. Sebak, "Spatially weighted numerical models for the two-dimensional wave equations: FD algorithm and synthesis of the equivalent TLM model," *Int. J. Numerical Modelling* , vol. 6, pp. 47–65, 1993.

[9] M. Celuch-Marcysiak and W. K. Gwarek, "New TLM algorithms with controlled stability margin and their application to improve the modelling of curved boundaries," in *IEEE MTT-S Dig.*, San Diego, 1994.
[10] W. K. Gwarek, "Analysis of an arbitrarily-shaped planar circuit—a time-domain approach," *IEEE Trans. Microwave Theory Tech.*, vol. MTT-33, no. 10, pp. 1067–1072, Oct. 1985.
[11] W. K. Gwarek and C. Mroczkowski, "Effective analysis of two-dimensional waveguide discontinuities," in *Int. Conf. Microwaves and Optoelectronics MIOP*, Wiesbaden, Germany, 1990, pp. 550–555.
[12] P. H. Harms, J.-F. Lee, and R. Mittra, "A study of the nonorthogonal FDTD method versus the conventional FDTD technique for computing resonant frequencies of cylindrical cavities," *IEEE Trans. Microwave Theory Tech.*, vol. 40, no. 4, pp. 741–746, Apr. 1992.
[13] A. Fettweis and G. Nitsche, "Numerical integration of partial differential equations using principles of multidimensional wave digital filters," *J. VLSI Signal Processing*, vol. 3, pp. 7–24, 1991.
[14] W. K. Gwarek, "Analysis of arbitrarily-shaped two dimensional microwave circuits by finite-difference time-domain method," *IEEE Trans. Microwave Theory Tech.*, vol. 36, no. 4, pp. 738–744, Apr. 1988.
[15] M. Celuch-Marcysiak, W. K. Gwarek, Z. Chen, M. M. Ney, and W. J. R. Hoefer, "Comments on 'A new finite-difference time-domain formulation and its equivalence with the TLM symmetrical condensed node' and reply to comments," *IEEE Trans. Microwave Theory Tech.*, vol. 41, no. 1, pp. 168–171, Jan. 1993.
[16] Z. Chen, M. M. Ney, and W. J. R. Hoefer, "A new finite-difference time-domain formulation and its equivalence with the TLM symmetrical condensed node," *IEEE Trans. Microwave Theory Tech.*, vol. 39, no. 12, pp. 2160–2169, Dec. 1991.
[17] M. Celuch-Marcysiak and W. K. Gwarek, "On the aspects of selecting the symmetrical condensed node or the expanded node modelling for electromagnetic simulations," *Eur. Microwave Conf. Dig.*, Helsinki, 1992.
[18] I. S. Kim and W. J. R. Hoefer, "Numerical dispersion characteristics and stability factor for the TD-FD method," *Electron. Lett.*, vol. 26, no. 7, pp. 485–487, Mar. 1990.
[19] D. Potter, *Computational Physics*, ch. 6. New York: Wiley, 1973.
[20] I. S. Kim and W. J. R. Hoefer, "The numerical energy conservation of the TD-FD method," *IEEE Trans. Magnetics*, vol. 27, no. 5, pp. 4056–4059, Sept. 1991.
[21] W. Gwarek and M. Celuch-Marcysiak, "Time-domain analysis of dispersive transmission lines," *Journal de Physique III*, France, pp. 581–591, Mar. 1993.

Malgorzata Celuch-Marcysiak was born in Warsaw, Poland, in 1964. She is a graduate of the United World Colleges. In 1988 she received the M.Sc. degree (honors) in electronic engineering from the Warsaw University of Technology. Currently she is working towards the Ph.D. degree at the Institute of Radioelectronics, Warsaw University of Technology.

Her current research interests are in the area of electromagnetic field theory and numerical analysis of microwave circuits, with emphasis on relationships between various numerical methods.

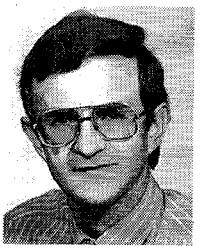

Wojciech K. Gwarek (SM'90) was born in Poland. He received the M.Sc. degree in 1974 from Massachusetts Institute of Technology, the Ph.D. degree in 1977, and Habilitation in 1988 from the Warsaw University of Technology, Warsaw, where he is currently a Professor.

In 1991 to 1992 he was a Visiting Professor at Ecole Nationale Superieure de Telecommunications de Bretagne, Brest, France. He also helped in organizing the Franco-Polish School of New Information and Communication Technologies in Poznan, Poland in 1992 to 1993. He is author of many scientific papers, a textbook on electromagnetic theory and a software package named QuickWave (distributed by ArguMens GmbH, Duisburg, Germany). His current research interests are in the areas of electromagnetic field theory and computer-aided analysis and design of microwave circuits.

Dr. Gwarek is a Member of Editorial Board of IEEE TRANSACTIONS ON MICROWAVE THEORY AND TECHNIQUES and a Member of the Technical Programme Committee of the European Microwave Conference.